Molecular evolution of male reproduction across species with highly divergent sperm morphology in diverse murine rodents

Emily E. K. Kopania[1,2,3], Gregg W. C. Thomas[1,4], Carl R. Hutter[5], Sebastian M. E. Mortimer[1], Colin M. Callahan[1], Emily Roycroft[6,7,8], Anang S. Achmadi[9], William G. Breed[10], Nathan L. Clark[2,3], Jacob A. Esselstyn[5], Kevin C. Rowe[6,7], Jeffrey M. Good[1]

[1] Division of Biological Sciences, University of Montana, Missoula, MT, USA
[2] Department of Human Genetics, University of Utah, Salt Lake City, UT, USA
[3] Department of Biological Sciences, University of Pittsburgh, Pittsburgh, PA, USA
[4] Informatics Group, Harvard University, Cambridge, MA, USA
[5] Department of Biological Sciences, Louisiana State University, Baton Rouge, LA, USA
[6] School of BioSciences, The University of Melbourne, Parkville, VIC, Australia
[7] Sciences Department, Museums Victoria, Melbourne, VIC, Australia
[8] Division of Ecology and Evolution, Research school of Biology, The Australian National University, Acton, ACT, Australia
[9] Museum Zoologicum Bogoriense, Research Center for Biology, Cibinong, Jawa Barat, Indonesia
[10] School of Biological Sciences and Robinson Research Institute, The University of Adelaide, Adelaide, SA, Australia

Keywords:
sperm, reproduction, murine rodents, sperm competition, phylogenetic comparisons

Sperm competition can drive rapid evolution of male reproductive traits, but it remains unclear how variation in sperm competition intensity shapes phenotypic and molecular diversity across clades. Old World mice and rats (subfamily Murinae) comprise a rapid radiation and exhibit incredible diversity in sperm morphology and production. We combined phenotype and sequence data to model the evolution of reproductive traits and genes across 78 murine species. We identified several shifts towards smaller relative testes mass, a trait reflective of reduced sperm competition. Several sperm traits were associated with relative testes mass, suggesting that mating system evolution likely selects for convergent traits related to sperm competitive ability. Molecular evolutionary rates of spermatogenesis proteins also correlated with relative testes mass, but in an unexpected direction. We predicted that sperm competition would result in rapid divergence among species with large relative testes mass, but instead found that many spermatogenesis genes evolve more rapidly in species with smaller relative testes mass due to relaxed purifying selection. While some reproductive genes evolved under positive selection, relaxed selection played a greater role underlying rapid evolution in small testes species. Our work demonstrates that sexual selection can impose strong purifying selection shaping the evolution of male reproduction.

Authors for correspondence:
Emily E. K. Kopania
email: emk270@pitt.edu
Jeffrey M. Good
email: jeffrey.good@umontana.edu

1. Introduction

Sperm competition often leads to the rapid evolution of male reproductive traits (1-5), which can drive both extreme phenotypic divergence within populations (1) and the evolution of reproductive barriers between nascent species (6). Rapid evolution of reproduction also occurs at the molecular level, with reproductive genes tending to show rapid protein sequence evolution (7-11). Rapid protein-coding divergence is often attributed to pervasive positive selection (7, 8), but other processes such as relaxed purifying selection may be common for tissue-specific male reproductive genes (12-16). However, the selective processes shaping broad patterns of molecular evolution and the connections between genotypic and phenotypic evolution remain elusive for male reproduction.

If sperm competition tends to select for particular reproductive traits, then interspecific divergence in these phenotypes should be correlated with the

intensity of sperm competition (3, 17-19). While directly quantifying sperm competition is challenging, some clades show a correlation between the intensity of sperm competition and relative testes mass (2, 5, 20, 21), thus providing a proxy for the intensity of sperm competition (4, 22). If sperm competition also drives rapid divergence of reproductive proteins, then genes underlying these proteins may also evolve more rapidly with more frequent positive selection in lineages with the most sperm competition. Consistent with these predictions, molecular evolution appears to be fastest for male reproductive genes expressed during key stages of sperm morphological development (23-25) and for secreted accessory components of the male ejaculate involved in male-female interactions and sperm competition (26). However, most studies have focused on relatively few species, and therefore have been underpowered to directly test for relationships between molecular and reproductive trait evolution.

The subfamily Murinae represents one of the most rapid mammalian radiations with >700 species (i.e., >10% of extant mammal species) arising over the last ~12-14 million years (11, 27, 28). Murines also show striking diversity in reproductive biology (11, 29), including extreme interspecific divergence in relative testes mass and sperm morphology [Figure 1; (30)]. The house mouse *(Mus musculus*) and Norway rat (*Rattus norvegicus*) model species are part of this radiation, providing extensive genomic resources (11, 31, 32) and a detailed understanding of murine spermatogenesis and reproductive biology (29, 33, 34). Previous studies suggest that some sperm morphological traits have evolved in response to sperm competition in murine rodents (4, 22), but these works relied on phylogenies that were not well-resolved or included relatively few species (4, 11, 35), thus limiting comparative analysis of murine rodent reproductive evolution.

Here, we use targeted exon enrichment to sequence 11,775 protein-coding genes across 36 murine species, combined with published exome (11, 36) and genome (31) data for 42 species, resulting in 78 sequenced species with available reproductive trait data. We address four main questions: (i) Does the intensity of sperm competition underlie variation in sperm head morphology in murines? (ii) Is there heterogeneity of molecular evolutionary rates among reproductive tissues and cell types across murines? (iii) What are the relative roles of positive selection and relaxed purifying selection in driving the molecular evolution of male reproductive genes? (iv) Are changes in the intensity of sperm competition associated with lineage-specific shifts in molecular evolutionary rates?

2. Results

(a) High quality assemblies and phylogeny of diverse murine rodents

We used exons from 11,775 protein-coding genes to generate assemblies, alignments, gene trees, and a species tree for 210 murine species, which will be reported in a forthcoming manuscript. Here, we report results for 78 species with both exome (n=77) or genome (n=1) sequences and male reproductive phenotypes plus two outgroups (Supplemental Table S1, Supplemental Table S2). Across the 77 exomes, about 89% of reads on average mapped to our de novo assemblies with an average depth of 22x. Based on *Referee* (37), our assemblies had on average fewer than 0.0005 errors per base and about 2% low quality positions, indicating that our assemblies were of high quality. The resulting pruned species tree (Figure 1) was well-supported, with one node having an ASTRAL support value of 0.93 and all other nodes having an ASTRAL support value of 1. However, concordance factors were more varied, with a median gene concordance factor of 38 and a median site concordance factor of 45.7, likely reflecting high levels of incomplete lineage sorting or introgression (38).

(b) Murine rodents show repeated shifts to smaller relative testes mass

Our findings suggest considerable variation in mating behavior and likely sperm competition (17), with several species groups independently evolving mating systems with lower levels of multiple mating. Relative testes mass ranged from 0.1% to 4.8% of body mass (Figure 1; Supplemental Table S2). The Ornstein-Uhlenbeck (OU) model identified four adaptive peaks corresponding to convergent phenotypic optima. Three peaks represented shifts to smaller relative testes mass (blue, orange, and brown; Figure 1) and one represented a shift to larger testes mass (purple; Figure 1). Because most shifts were to smaller testes mass, we focused on small testes as our foreground trait. OU models can be prone to errors in estimates of adaptive peaks (39), and we found that the number of adaptive peaks for species with small testes mass was sensitive to model selection (Supplemental Figure S1). Indeed, one of these adaptive shifts (blue, Figure 1) had inconsistent species membership across different model selection methods (Supplemental Figure S1), represented a small phenotypic optimum, and included *Mus musculus*, which experiences intense sperm competition in natural populations (40). Given these considerations, we focused on the two groups with the most pronounced phenotypic shifts (i.e., orange and brown groups denoted by † in Figure 1) as representing murines with the lowest relative levels of sperm competition. These groups were combined as one “low sperm competition” group for further analyses.

(c) Sperm competition selects for longer sperm hooks, narrower heads, and longer tails

We used phylogenetic logistic regression [binary traits; (41)] or phylogenetic generalized least squares (42) to test if sperm morphology traits were correlated with relative testes mass. We found that hook presence was positively associated with relative testes mass (FDR-corrected $P < 0.01$; Figure 2A). We ran phylogenetic generalized least squares using Brownian motion, Pagel’s λ (43), and an OU model (42). With all three models, we found significant associations between relative testes mass and hook length, hook angle, ventral process length, ventral process angle, head width, tail length, and principal and end piece length (FDR-corrected $P < 0.05$; Figure 2; Supplemental Figure S2; Supplemental Table S3). Sperm head width was negatively associated with relative testes mass (FDR-corrected $P < 0.01$; Figure 2E), suggesting that sperm competition selects for narrower

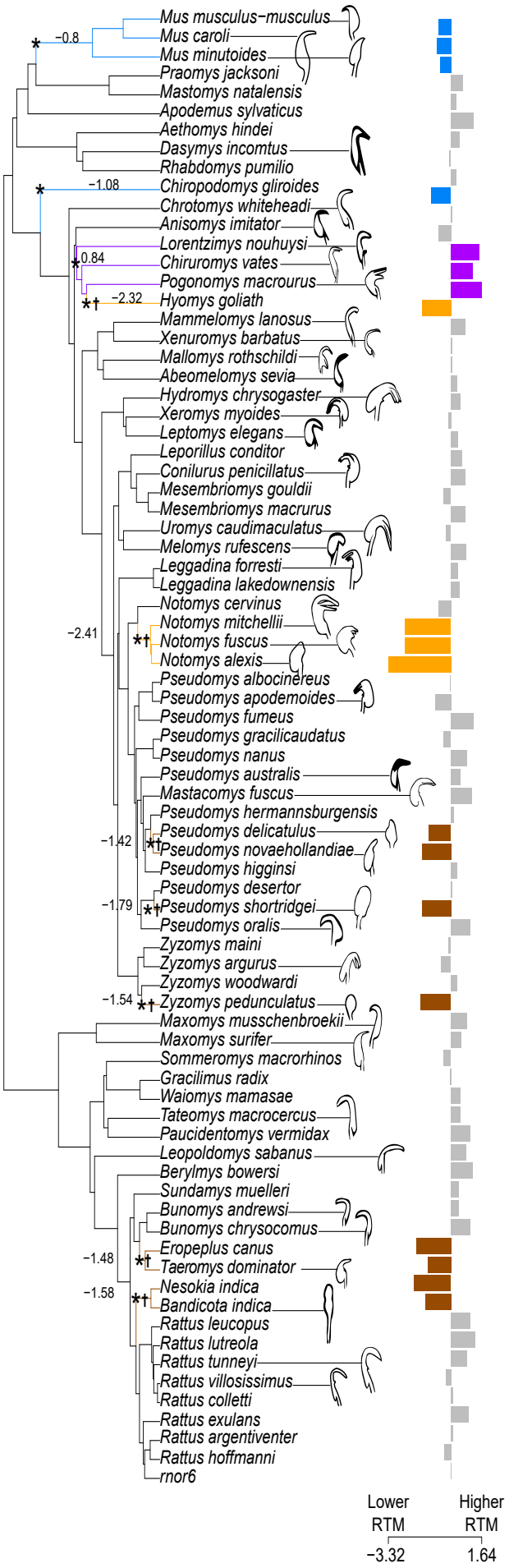

Figure 1. Phylogenetic variation in testes mass and sperm morphology across 78 murine species. Bar plots show normalized values of relative testes mass, with different colors representing distinct adaptive peaks based on an OU model. Blue, orange, and brown bars indicate shifts to smaller testes while purple bars indicate shifts to larger testes. (*) indicate phylogenetic nodes corresponding to shifts in phenotypic optima, and adjacent values show optimum trait values at these nodes. (†) show lineages used as foreground small testes species for downstream analyses. Traces of sperm micrographs (not to scale) are shown for some species to highlight the diversity of sperm head morphology.

sperm heads with faster swimming speed (44). Sperm head length and sperm head area were correlated with relative testes mass under some models (Supplemental Figure S2; Supplemental Table S3). Collectively, these data reveal correlated evolution across traits that are likely relevant to sperm competitive ability and, to the extent that relative testes mass is a robust proxy of sperm competition, reflect phenotypic evolution in response to lineage-specific variation in the intensity of sperm competition.

(d) Rapid evolution of genes enriched in late spermatogenesis and seminal vesicles

Next, we evaluated molecular evolution across different components of male reproduction. Using proteomics data (26), we calculated rates of protein-coding evolution (d_N/d_S) for genes grouped based on the male accessory tissue (seminal vesicles, coagulating gland, dorsolateral prostate, ventral prostate, bulbourethral gland, bulbourethral diverticulum) in which their encoded proteins were detected at the highest level. We also estimated an average d_N/d_S for genes with testis-specific expression patterns in house mice (16). Most male reproductive tissues had average d_N/d_S values similar to or lower than the genome-wide average (Table 1; Figure 3A), suggesting protein sequence conservation (26). However, seminal vesicle genes tended to evolve rapidly (d_N/d_S = 0.26; Table 1; Figure 3A; FDR-corrected Wilcoxon rank-sum $P < 0.05$). The three genes enriched in the coagulating gland also had a high median d_N/d_S (0.35), but this was not significantly different from the genome-wide average (Table 1). The median d_N/d_S of all genes detected in the seminal vesicles was not significantly higher than the genome-wide average (Supplemental Table S4), suggesting that the more rapid divergence was limited to genes specialized to this tissue. Testis-specific genes had an average d_N/d_S of 0.20, higher than the genome-wide average (Figure 3A; FDR-corrected Wilcoxon rank-sum test $P < 0.05$).

To test for variation in evolutionary rates across spermatogenesis, we compared d_N/d_S for genes associated with testis somatic cells, diploid spermatogonia, early meiosis (pre-leptotene), meiotic spermatocytes, postmeiotic spermatids, and elongating spermatids (Figure 3; Table 1) based on single-cell RNAseq data from house mice (33). Genes enriched in early and middle spermatogenesis stages (spermatogonia, pre-leptotene, and spermatocytes) had median d_N/d_S less than, or similar to, that of the genome-wide av-

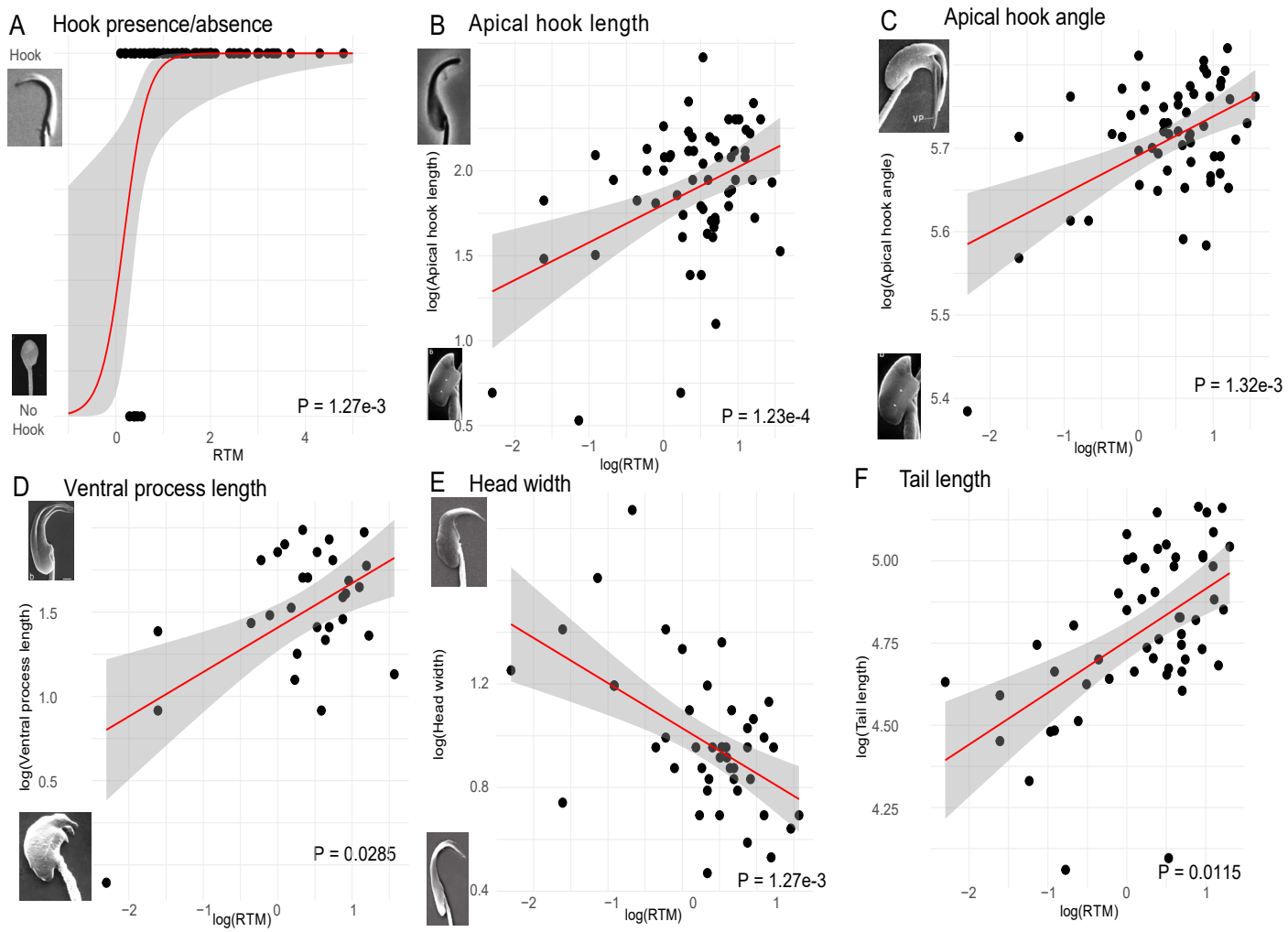

Figure 2. Correlations between relative testes mass (RTM) and sperm morphology traits. Red lines and gray areas show regressions and confidence intervals based on a logistic regression (A) or generalized linear models (B-F). P-values are based on phylogenetic logistic regression (A) or phylogenetic generalized least squares analyses using a Brownian motion model (B-D) with Benjamini-Hochberg correction for multiple tests. All lengths and widths were measured in µm, angles were measured in degrees, and relative testes mass was measured as a percent of body mass. Sperm micrographs show examples of the extreme ends of each trait along the y-axis (sources in Supplemental Table S3).

erage, while genes enriched during the postmeiotic spermatid and elongating spermatid stages showed higher d_N/d_S (Table 1; Figure 3A; FDR-corrected Wilcoxon rank-sum tests P < 0.05). These results suggest that more rapid protein sequence divergence in late spermatogenesis underlies rapid divergence of testis genes, consistent with results for both closely related mouse lineages (23, 45) and more broadly across mammals (24).

(e) Both positive selection and relaxed purifying selection contributed to the rapid divergence of some reproductive genes

The rapid evolution of genes enriched in seminal vesicles and during late spermatogenesis may result from relaxed purifying selection, positive directional selection, or both. For the seminal vesicles, 17% of genes showed evidence for positive selection based on the codeml site test [M1a vs M2a; (48)], compared to the genome-wide average of 11%, but this difference was not significant (FDR-corrected P > 0.05; Table 1; Supplemental Figure S3). Similarly, rapidly evolving round spermatids and elongating spermatids had nominally higher proportions of genes with evidence for positive selection than other spermatogenesis cell types, but this difference was not significant (Figure 3B; Table 1; Pearson's chi-squared FDR-corrected P > 0.05). Both contrasts relied on relatively small sample sizes, limiting statistical power.

Many male reproductive genes are highly tissue- or cell-type-specific, leading to the prediction that they may be under relaxed purifying selection. We identified the proportion of cell-type-enriched genes that were testis-specific to estimate the degree to which relaxed constraint may shape molecular evolution across spermatogenesis stages. Early-stage diploid spermatogonia had proportionally fewer testis-specific genes, whereas mid- to late-stage spermatogenesis cell types had proportionally more testis-specific genes (Figure 3C; Table 1; FDR-corrected Pearson's chi-squared P < 0.05). Genes enriched in round spermatids had the highest proportion that were testis-specific (Figure 3C; Table 1). Positive selection and relaxed purifying selection are not mutually exclusive, and testis-specific genes may be freer to diverge rapidly under positive selection because they are

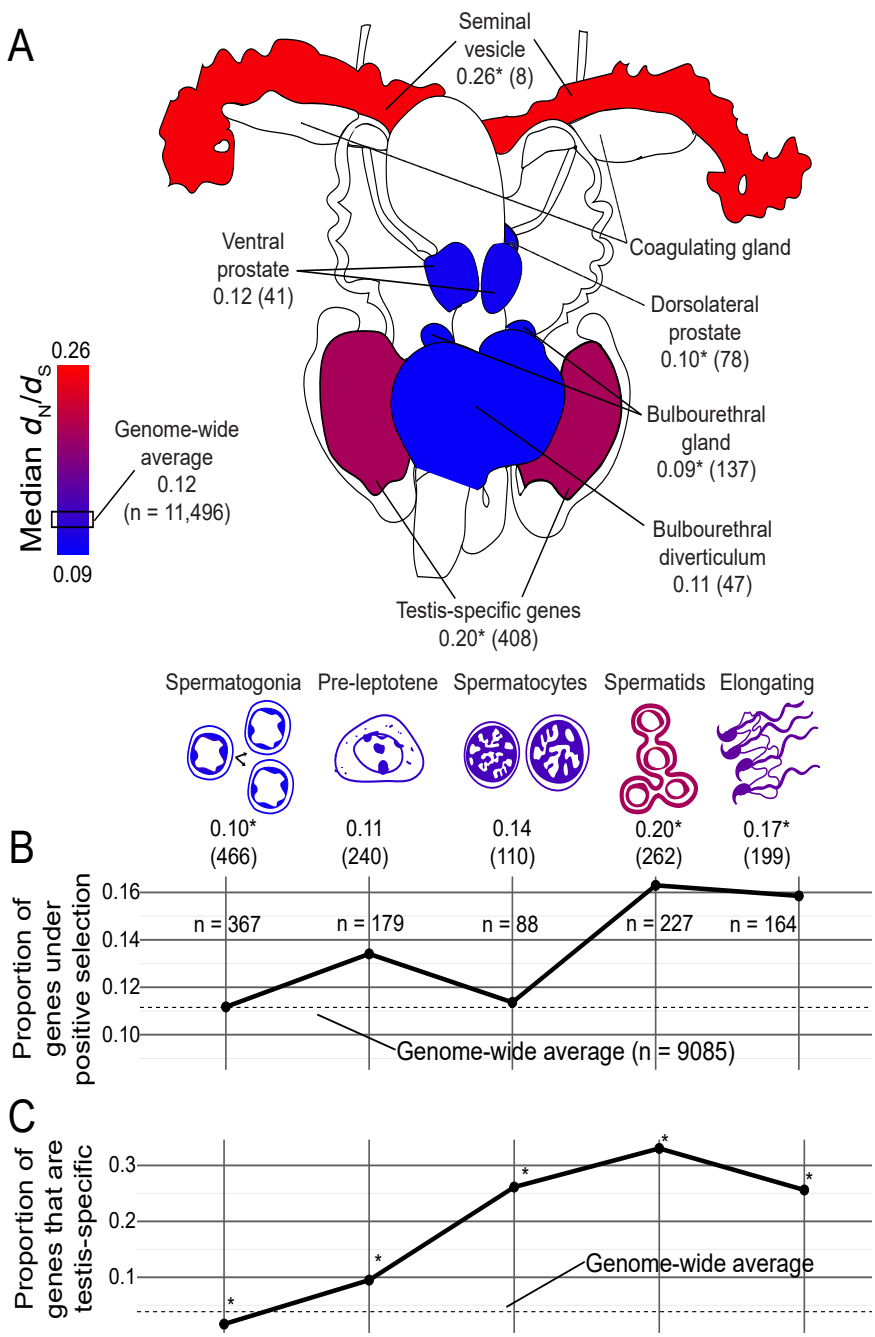

Figure 3. Molecular evolution by male reproductive tissue and spermatogenesis stage. (A) Mouse male reproductive tract and spermatogenesis cell types ordered from earliest to latest developmental stages. Numbers represent median d_N/d_S values for each tissue or cell type with gene counts in parentheses. Coagulating gland was excluded because data were only available for three genes in this tissue. The box on the scale indicates the median phylogeny-wide d_N/d_S (0.12) across all genes, and (*) indicate significant differences from this median d_N/d_S (Wilcoxon rank sum test FDR-corrected P < 0.05). (B) Proportion of genes enriched in each cell type with evidence for positive selection alongside the proportion of genes with evidence for positive selection out of all genes included in the test for selection (dotted line; all cell types were not significantly different at an FDR-corrected Pearson's chi-squared P > 0.05). (C) Proportion of genes enriched in each cell type that were testis-specific, with (*) indicating significance as above. Figure concept and male reproductive tract outline in (A) adapted from (26), the pre-leptotene cell was traced from (46), and all other cell images were adapted from (47).

not constrained by functions in other tissues (24). Consistent with this, a significantly higher percentage of testis-specific genes were under positive selection compared to the genome-wide average (testis-specific: 22%; genome-wide: 11%; FDR-corrected P < 0.01; Table 1).

(f) Spermatogenesis genes showed accelerated evolutionary rates in species with low levels of sperm competition, largely due to relaxed purifying selection

We next used *RERconverge* (49) with small testes mass species as foreground branches (Figure 1, orange and brown groups denoted by †) to test if changes in the intensity of sperm competition were associated with lineage-specific shifts in molecular evolution. Of 11,597 genes, five showed significantly accelerated evolutionary rates after correcting for multiple tests (positive *RERconverge* Rho values; FDR-corrected P < 0.05; Table 2). We also looked for functional enrichment among the most accelerated genes based on *RERconverge* p-values (Supplemental Table S5). The 10 most accelerated genes had known functions in reproduction or were highly expressed in the testes (Table 2). The top 250 most accelerated genes were significantly enriched for the "male gamete generation", "spermatogenesis", and "gamete generation" gene ontology (GO) terms (Figure 4; Supplemental Table S6; FDR-corrected P < 0.01). Only genes accelerated in small testes species were enriched for the spermatogenesis GO term (Figure 4A). To ensure that this result was statistically robust, we used a combination of phylogenetic permutations and simulations [i.e., permulations (50)] and found that terms related to reproduction were still among the most significantly enriched GO terms (Supplemental Table S6).

We also ran *RERconverge* with different sets of foreground species, including with large relative testes mass

Table 1. Summary of molecular evolution by spermatogenesis stage and male reproductive tissue. (*) indicate significant differences from the average of all genes (FDR-corrected P < 0.05). SO = somatic; SG = spermatogonia; PL = pre-leptotene; SC = spermatocytes; SD = spermatids; EL = elongating; BD = bulbourethral diverticulum; BG = bulbourethral gland; CG = coagulating gland; DP = dorsolateral prostate; VP = ventral prostate; SV = seminal vesicle; TS = testis-specific

	All Genes	Spermatogenesis cell types (33)						Male reproductive tissues						
	All Genes	SO	SG	PL	SC	SD	EL	BD (26)	BG (26)	CG (26)	DP (26)	VP (26)	SV (26)	TS (16)
Number of genes (d_N/d_S)	11496	60	466	240	110	262	199	47	137	3	78	41	8	408
Median d_N/d_S	0.12	0.08*	0.10*	0.11	0.14	0.20*	0.17*	0.11	0.09*	0.35	0.10*	0.12	0.26*	0.20*
Number of genes	9085	45	367	179	88	227	164	39	110	2	60	34	6	350
Percent of genes under positive selection	11%	8.9%	11%	13%	11%	16%	16%	13%	7%	0%	8.3%	8.8%	17%	22%*
Percent of testis-specific genes under positive selection	22%	0%	17%	35%	22%	21%	19%	NA	NA	NA	NA	NA	NA	NA
Percent of genes that are testis-specific	3.9%	4.4%	1.6%*	9.5%*	26%*	33%*	26%*	NA	NA	NA	NA	NA	NA	NA

(highest 10%) species as foreground, and with relative testes mass as a continuous trait. For the continuous trait model, we also found that spermatogenesis genes and testis-specific genes were accelerated in smaller testes species (Supplemental Figure S4). When we assigned foreground branches based on large testes mass species, neither accelerated nor decelerated genes were enriched for spermatogenesis genes or testis-specific genes (Supplemental Figure S4). Overall, these comparisons suggest that relaxed purifying selection in low sperm competition species, rather than positive selection in species with high sperm competition, may make a larger contribution to interspecific variation in evolutionary rates of spermatogenesis genes in murines. To test this hypothesis, we tested for positive selection acting on spermatogenesis genes on branches leading to small testes species using a branch-site test in codeml. We also compared the branch-site null model to the M1a model to test for relaxed purifying selection in these lineages (51). We found evidence for relaxed purifying selection acting on 39 spermatogenesis genes in small testes species, and the majority of these were accelerated in small testes species (Figure 4A, teal tick marks; Supplemental Table S5). When looking only at genes with evidence for relaxed purifying selection, we saw a stronger enrichment for the spermatogenesis GO category among genes accelerated in small testes species (Figure 4B). In contrast, only 11 spermatogenesis genes showed evidence for positive selection in small testes species, and these were spread across the range of *RERconverge* output values rather than concentrated at the accelerated end (Figure 4A, red tick marks). Spermatogenesis genes under phylogeny-wide positive selection also were not enriched for acceleration or deceleration in small testes species (Figure 4A, purple tick marks).

3. Discussion

Many of the most remarkable examples of rapid phenotypic and molecular evolution are related to male reproduction (1, 3, 56, 57), but few studies have directly tested how interspecific differences in inferred post-mating sexual selection pressures act on both phenotypic and molecular evolution. Our dataset consisting of genomic and phenotype data from 78 murine species allowed us to address this in a rigorous phylogenetic framework.

(a) The evolution of male reproductive phenotypes in murines

We found evidence for the repeated evolution of smaller testes, suggesting that most murines have a high frequency of female multiple mating but with repeated shifts to mating systems with less frequent female remating (Figure 1). We also identified several sperm morphological traits associated with relative testes mass (Figure 2). Our findings suggest that sperm competition selects for the presence of a hook, as well as longer and more angled hooks (4, 58, 59). Compared to a previous study that sampled fewer murine species with less sperm diversity (4), we found consistent support that relative testes mass is associated with hook morphology and sperm tail length, but in contrast we did not find an association with sperm head area.

Our data suggest that sperm hook evolution is relevant to sperm competition in murines, but hook function and its role in post-copulatory sexual selection remains a mystery. In some species, the hooks attach sperm from the same male

Table 2. The top 10 most accelerated genes in small relative testes mass species based on *RERconverge*. Higher Rho values indicate a stronger positive correlation between relative molecular evolutionary rate and small testes mass. P.adj is the p-value from *RERconverge* corrected for multiple tests. Expression patterns are based on the Bgee suite (52). Reproductive functions are based on Uniprot (53) and the Mouse Genome Informatics database unless noted otherwise.

Gene symbol	Rho	P.adj	Expression Patterns	Reproductive Function
Zcchc13	0.3548	8.35E-03	High in testis	Homozygous mutants show normal fertility
Stk31	0.3386	8.35E-03	Highest in spermatocyte; also highly expressed in other gonadal and zygotic tissues	Homozygous mutants show normal fertility
Akap4	0.3171	3.98E-02	Testis-specific (especially spermatid)	Part of sperm fibrous sheath structure; involved in sperm motility
Sel1l2	0.3537	4.16E-02	Highly expressed in spermatid, spermatocyte, and seminiferous tubules	Unknown
Ppp2r1b	0.3129	4.16E-02	Expressed in several developing tissues, including indifferent gonad; also expressed in seminal vesicle and spermatid	Essential for proper meiosis in spermatocytes; homozygous deletion mice infertile (54)
Sox30	0.2837	6.30E-02	High in testis	Activates postmeiotic genes involved in spermiogenesis
Ddx43	0.2651	1.37E-01	Highest in spermatocyte; also highly expressed in other gonadal and zygotic tissues	Chromatin remodeling; homozygous deletion mice infertile (55)
Calr3	0.2706	1.70E-01	Highest in spermatid; also highly expressed in other gonadal and zygotic tissues	Required for zona pellucida binding and fertilization
Angel1	0.2658	1.70E-01	Highest in spermatid; also highly expressed in other gonadal and zygotic tissues	Unknown
Ybx2	0.2739	1.74E-01	Highest in seminiferous tubule; also highly expressed in other gonadal and zygotic tissues	Required for late stages of spermatogenesis; required for both male and female fertility

to form sperm trains, which speed the transfer to the egg (60). This was thought to be the main function of the hook (59), but other work has revealed that many species rarely form sperm trains, and trains that do form disaggregate quickly and do not show increased swimming speed or fertilization success (61-63). Alternatively, hooks may improve sperm swimming speed (58) or attach to the female reproductive tract to avoid being flushed out (61). The hook also contains part of the acrosome, which contains enzymes that break down the zona pellucida egg coat layer, and therefore could mediate sperm-egg interactions (56, 64).

It was not feasible to directly measure levels of sperm competition for most species in our dataset, so we used relative testes mass as a proxy for the intensity of sperm competition. There is a direct correlation between the intensity of sperm competition and relative testes mass in many vertebrate species (2, 5, 20, 21), including some murines (5, 20). However, this correlation may not hold for all taxa, because testes perform functions beyond sperm production, and changes in testes architecture can lead to increased sperm production without increased testes size (65, 66). Furthermore, some large testes species display behaviors associated with monogamy, such as biparental care in *Mus spretus* (67). Relative testes mass also may not reflect other components of post-mating sexual selection that influence sperm morphology, such as cryptic female choice (68). For example, cryptic female choice may also act on sperm hook morphology, especially if the hook is involved in interactions with the female reproductive tract (61).

(b) The relationship between phenotypic and molecular evolution in response to sperm competition

We showed that the rapid molecular divergence of male reproduction in murine rodents primarily occurred in testis-specific genes, and genes enriched in the seminal vesicles and postmeiotic spermatogenesis cell types, consistent with previous studies [Figure 3; Table 1; (23-26)]. The seminal vesicles contain secretions involved in copulatory plug formation, which is important for fertilization success and to limit female remating (26, 69), and are also enriched for immune function genes (26), which evolve rapidly in primate ejaculates (70) and in murine rodents (11). Postmeiotic spermatogenesis genes may be subject to positive directional selection on diverse aspects of sperm head morphology [(1); Figure 2], which develops during the later postmeiotic stages.

Previous studies have shown strong evidence for positive selection acting on a subset of reproductive genes, which plays an important role in their overall rapid divergence (7-11), but relaxed pleiotropic constraint likely also plays an important role in the rapid divergence of reproductive genes (12, 23-26). We did not find significantly higher proportions of genes under positive selection in the rapidly evolving seminal vesicles and postmeiotic spermatids (Table 1). This

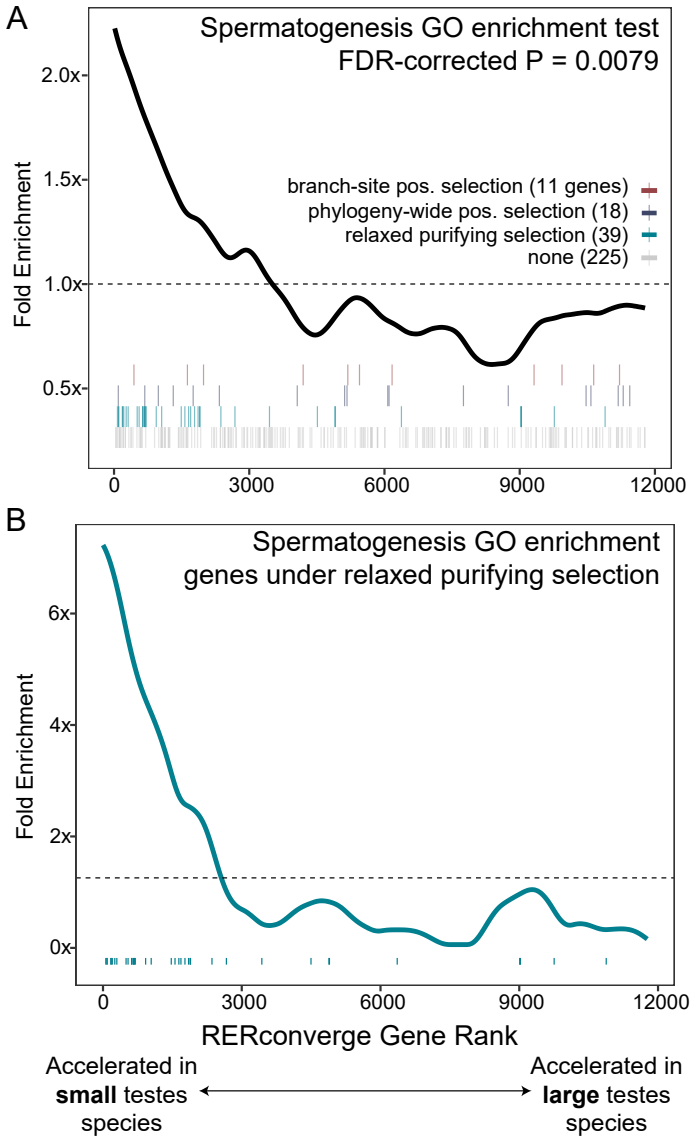

Figure 4. Enrichment for genes in the spermatogenesis GO category based on *RERconverge* rank. The x-axis indicates every gene included in the *RERconverge* analysis, ordered by their correlation score. The worm indicates enrichment for genes in the spermatogenesis GO category in windows along the x-axis. The horizontal dashed line is at 1x and therefore represents no over- or under-enrichment. Each tick mark indicates a gene in the spermatogenesis GO category, colored based on evidence for selection. The placement of ticks on the y-axis is arbitrary. (A) Enrichment for the spermatogenesis GO category, with p-value indicating significant enrichment for the spermatogenesis GO category among the 250 most significantly accelerated genes. (B) Enrichment for genes in the spermatogenesis GO category for genes with evidence for relaxed selection [i.e., genes represented by teal tick marks in (A)].

may be in part because some rapidly evolving genes were filtered out during assembly and alignment (see Methods), including many genes secreted by the seminal vesicles and known to be under positive selection in house mice (71) and primates (8). Regardless, relaxed purifying selection and positive selection are not mutually exclusive, and the relaxation of purifying selection may allow for the rapid fixation of mutations under positive selection [Table 1; (14)].

We predicted that lineages with a higher intensity of sperm competition would show more rapid molecular evolution of reproductive genes due to positive directional selection. However, we found the opposite pattern, with spermatogenesis and testis-specific genes tending to evolve more rapidly in small testes species (Figure 4A; Supplemental Figure S4). The top ten most accelerated genes in small testes species are all highly expressed in house mouse testes (52), and some have known essential functions in house mouse male fertility (Table 2). However, others do not affect fertility in mouse mutational studies or have known functions in reproduction (e.g., *Zcchc13, Stk31, Sel1l2, Angel1*), and therefore provide candidates for future studies investigating male fertility in the context of sperm competition.

We showed that rapid divergence in small testes species was largely due to relaxed purifying selection in these lineages (Figure 4B). Although sperm competition is typically assumed to be associated with positive selection, our results suggest that sperm competition also influences the intensity of purifying selection on many genes, and that shifts in these pressures can be a major driver of molecular evolution. This has been predicted theoretically (72), but rarely shown empirically at the molecular level (but see 73). Strong purifying selection on spermatogenesis genes in large testes species is also consistent with phenotypic observations. For example, there is a negative correlation between intraspecific variation in sperm morphology and relative testes mass in rodents and passerine birds, suggesting that sperm competition pressures may reduce variation in sperm morphology (58, 74). In the small testes murine species *Notomys alexis* and *N. fuscus*, there is high intraspecific variation in sperm hook morphology, with some having small hooks or ventral processes and others lacking these structures altogether (75). Thus, sperm competition may impose purifying selection on genes involved in sperm development to facilitate a higher proportion of high-quality sperm in the ejaculate. We suggest that this represents a more complete understanding of the molecular evolution of reproductive genes, in which a small subset of genes evolve rapidly due to positive directional selection, while many others are highly conserved in lineages with intense sperm competition due to strong purifying selection imposed by post-mating sexual selection pressures.

4. Methods

(a) Samples and data collection

We combined data from multiple sources for a total of 78 species representing all the major tribes within Murinae (Supplemental Table S1). We sampled 36 specimens from museum and personal loans. We extracted DNA using a Qiagen DNeasy kit with modifications to account for tissue preservation [Supplemental Methods; (76, 77)]. We performed library preparation using a Kapa Biosystems HyperPrep Kit (Roche Diagnostics Corporation, Indianapolis, IN) and exome capture using custom SeqCap EZ Developer Probes (Roche Diagnostics Corporation, Indianapolis, IN)

targeting 203,188 exon regions (mm9 annotation). Pooled libraries were sequenced on Illumina NextSeq at HudsonAlpha Institute for Biotechnology, HiSeq 4000 at the University of Oregon, and HiSeqX at Novogene. For Australian samples, libraries were prepared using a modified Meyer & Kircher protocol (78), following the methods described in Roycroft et al. (36, 79) and sequenced on an Illumina HiSeq 2500 at the Australian National University's Biomolecular Resource Facility. We used liftOver to transfer the coordinates for targeted regions to match the mm10 reference genome (80). We also used data from 41 published exomes (11, 36) and the *Rattus norvegicus* reference assembly [rnor6; (31)]. Phenotypic data were compiled from several publications (Supplemental Table S2; Supplemental Methods).

(b) Assembly, alignment, and phylogenetic inference

This study was part of a more extensive phylogenomics analysis of 210 murine species. Here we focus on the subset of these species with sufficient reproductive data, and analysis of the full dataset will be reported elsewhere. We performed *de novo* exome assembly on samples from 210 species using SPAdes (81) and assessed assembly quality and corrected low-quality bases using *Referee* (37). We re-mapped reads to the corrected assemblies to genotype each sample. Exome assemblies were annotated using transcripts from mouse (mm10) and rat (rnor6) reference genomes that exist in both references as one-to-one orthologs with an Ensembl orthology confidence of 1 and have an d_S value <0.5 between mouse and rat. When multiple transcripts passed the first two filters, we kept the one containing the most probe targets.

To generate alignments, we first identified homologous regions between mouse reference exons and our assembled contigs using BLAST. We then converted mouse reference exons to trimmed amino acid sequences to keep coding sequences between exons in-frame, and we used exonerate (82) to identify exons in our assembled contigs that were homologous to mouse reference exons. We filtered out exons with fewer than 175 samples with a matching BLAST hit and aligned the remaining exons using MAFFT (83). We then back-translated to nucleotide sequences and filtered out sequences that were >20% gaps and had alignment sites in 3-codon windows in which 2 or more codons had 2 or more gaps in over half of the sequences or premature stop-codons. After filtering, our alignments had on average > 150 aligned sequences per protein, and the average non-gapped sequence length per protein was about 250 codons. Our final dataset included 188 species and 11,775 protein-coding genes. From these alignments, we inferred gene trees using IQtree v2.0.4 (84, 85) with 1000 bootstrap iterations (86) and inferred a summary species tree from the gene trees using ASTRAL-MP v5.15.2 (87). We estimated branch lengths in terms of relative number of substitutions on the ASTRAL species tree using loci whose inferred gene tree had a normalized Robinson-Foulds distance to the species tree of less than 0.25 to minimize the effects of incomplete lineage sorting on branch length estimation (88). We then pruned this summary species tree using *ape* (89) to generate a species tree with 78 taxa that had male reproductive phenotype data (Figure 1).

(c) Phylogenetic analyses of trait evolution

We modeled the evolution of relative testes mass using an OU model implemented in *l1ou* v1.43 and identified convergent shifts in phenotypic optima using the function *estimate_convergent_regimes* with *criterion*="AIC" and *method*="rr" (90). We tested if sperm morphology parameters were significantly associated with relative testes mass using phylogenetic logistic regression (41) in *phylolm* v2.6.2 (91) for binary sperm hook presence/absence or phylogenetic generalized least squares in *nlme* v3.1.160 (92) for all other traits. We evaluated three different correlation structures: Brownian motion, Pagel's λ (43), and an OU model (42). We did not have all phenotype data for all species, so we pruned the tree for each trait to only include taxa with phenotype data for that trait (Supplemental Table S3). We used R v4.1.1 for all trait evolution analyses.

(d) Molecular evolution

We used codeml in PAML 4 (48) to calculate rates of protein sequence evolution (d_N/d_S; M0 model) and test for positive selection (M1a vs M2a) using gene trees pruned to include only species with reproductive phenotype data (Figure 1) and two outgroups (*Lophuromys woosnami* and *Lophiomys imhausi*). Running molecular evolutionary analyses on this full dataset would have required unreasonable runtimes, so we pared the species tree down to a subset of 41 taxa using a custom tree paring algorithm, *Bonsai* (https://github.com/gwct/bonsai), that prunes a phylogenetic tree so as to maximize branch lengths (Supplemental Methods). We tested if molecular evolutionary rates varied across accessory male reproductive tissues based on *Mus musculus* protein mass spectrometry data reported by (26). Testes were not included in this proteomics dataset, so we identified testis-specific genes using gene expression data from (16). We also compared d_N/d_S for genes enriched for expression across different testes cell types using *Mus musculus* single-cell RNA-seq data from (33). See Supplemental Methods for details. We then calculated median d_N/d_S values across all genes in each of these tissue- or cell type-associated gene sets and compared these values to the genome-wide median d_N/d_S using a Wilcoxon rank sum test with Benjamini-Hochberg correction for multiple tests. We then compared the proportions of genes with evidence for selection for these gene sets to the genome-wide average. For spermatogenesis cell types, we also calculated the proportion of genes enriched in each cell type that were considered testis-specific in (16). From these lists of genes associated with reproductive tissues or cell types, 1119 genes were excluded because they did not pass filtering.

We next used *RERconverge* (49) to identify genes showing relative molecular evolutionary rates shifts across lineages associated with convergent transitions to small testes mass. We set species consistently identified as having significant shifts to smaller testes in our OU models as foreground species (Figure 1). We verified results from *RERconverge* using 1000 permutations of phylogenetic simulations [i.e., permulations; (50)] with a Benjamini-Hoch-

berg correction for multiple tests. We then used *topGO* (93) to test for GO term enrichment among the top 250 most accelerated genes. We tested for episodic positive selection or relaxed purifying selection on reproductive genes in small testes species with branch-site tests in codeml (48). For each gene, we used a chi-squared test to compare the log likelihoods of the inferred branch-site model versus the branch-site null model (48). We also used a likelihood ratio test to compare the branch-site null model to the M1a model, with a higher likelihood of the null model considered evidence for relaxed purifying selection acting on foreground branches (48, 51).

Data accessibility. Exome data and assemblies are available at accession XXXXXXX. Raw sequence reads for all samples generated by Bioplatforms Australia are available from BPA Data Portal as part of the Oz Mammals Genomics Initiative using Library IDs provided in Supplemental Table S1 (https://data.bioplatforms.com). Scripts for assembly, alignment, and phylogenetic inference are available at https://github.com/goodest-goodlab/murinae-seq/tree/master. Scripts for all other analyses, the pruned 78 species tree, and lists of genes associated with reproductive tissues and cell types are available at https://github.com/ekopania/murine-sperm-analyses/tree/main.

Author Contributions. J.A.E., K.C.R., and J.M.G. conceived the project. A.S.A., J.A.E., and K.C.R. collected specimens. S.M.E.M., C.M.C., and E.J.R. collected the genomic data. W.G.B. and E.E.K.K. compiled the phenotypic data. G.W.C.T. and C.R.H. performed the assembly, alignment, and phylogenetic inference. E.E.K.K. analyzed the data with support from N.L.C. N.L.C., J.A.E., K.C.R., and J.M.G. funded the project. E.E.K.K. and J.M.G. wrote the manuscript with input from all authors.

Conflict of interest declarations. We declare we have no competing interests.

Funding. This work was funded by the NSF (DEB-1754096 and 1754393 to J.A.E., K.C.R., and J.M.G., and DGE-1313190 to E.E.K.K.), the NHGRI (R01-HG009299 to N.L.C.), and the NICHD (R01-HD073439 and R01-HD094787 to J.M.G.). This work was conducted using resources from the University of Montana Genomics Core supported by a grant from the M.J. Murdock Charitable Trust (to J.M.G.), the University of Montana Griz Shared Computing Cluster supported by grants from the NSF (CC-2018112 and OAC-1925267, J.M.G. co-PI), and the University of Utah Center for High Performance Computing partially funded by the NIH Shared Instrumentation Grant (1S10OD021644-01A1). We acknowledge the contribution of the Oz Mammals Genomics Initiative consortium in the generation of data used in this publication (https://ozmammalsgenomics.com/consortium/). The initiative is supported by funding from Bioplatforms Australia through the Australian Government National Collaborative Research Infrastructure Strategy (NCRIS). Any opinions, findings, and conclusions or recommendations expressed in this material are those of the authors and do not necessarily reflect the views of the NSF or the NIH.

Acknowledgements. We thank the Good and Clark labs, Doug Emlen, Lila Fishman, Erica Larson, and Travis Wheeler for helpful feedback on this study. We thank Ana Paula A Assis for assistance with the OU models. We thank the Museum of Vertebrate Zoology, Field Museum of Natural History, Louisiana State University Museum of Natural Science, Western Australia Museum, South Australia Museum, University of Kansas Biodiversity Research Center, Australian Biological Tissue Collection, Museum and Art Gallery of the Northern Territory, University of Canberra, Queensland Museum, Muséum National d'Histoire Naturelle, Museums Victoria, and Priscilla Tucker for providing tissue samples.

References

1. Pitnick S, Hosken DJ, Birkhead TR. Sperm morphological diversity. In: Birkhead TR, Hosken DJ, Pitnick S, editors. Sperm Biology. London: Academic Press; 2009. p. 69-149.
2. Harcourt AH, Harvey PH, Larson SG, Short RV. Testis weight, body weight and breeding system in primates. Nature. 1981;293:55.
3. Lüpold S, Manier MK, Puniamoorthy N, Schoff C, Starmer WT, Luepold SHB, et al. How sexual selection can drive the evolution of costly sperm ornamentation. Nature. 2016;533(7604):535-8.
4. Pahl T, McLennan HJ, Wang Y, Achmadi AS, Rowe KC, Aplin K, et al. Sperm morphology of the Rattini - are the interspecific differences due to variation in intensity of intermale sperm competition? Reprod Fertil Dev. 2018;30(11):1434-42.
5. Ramm SA, Parker GA, Stockley P. Sperm competition and the evolution of male reproductive anatomy in rodents. Proceedings of the Royal Society B: Biological Sciences. 2005;272(1566):949-55.
6. Manier Mollie K, Lüpold S, Belote John M, Starmer William T, Berben Kirstin S, Ala-Honkola O, et al. Postcopulatory Sexual Selection Generates Speciation Phenotypes in Drosophila. Curr Biol. 2013;23(19):1853-62.
7. Swanson WJ, Yang Z, Wolfner MF, Aquadro CF. Positive Darwinian selection drives the evolution of several female reproductive proteins in mammals. Proceedings of the National Academy of Sciences. 2001;98(5):2509-14.
8. Clark NL, Swanson WJ. Pervasive Adaptive Evolution in Primate Seminal Proteins. PLoS Genet. 2005;1(3):e35.
9. Ahmed-Braimah YH, Unckless RL, Clark AG. Evolutionary Dynamics of Male Reproductive Genes in the Drosophila virilis Subgroup. G3-Genes Genom Genet. 2017;7(9):3145-55.
10. Dean R, Wright AE, Marsh-Rollo SE, Nugent BM, Alonzo SH, Mank JE. Sperm competition shapes gene expression and sequence evolution in the ocellated wrasse. Mol Ecol. 2017;26(2):505-18.
11. Roycroft E, Achmadi A, Callahan CM, Esselstyn JA, Good JM, Moussalli A, et al. Molecular Evolution of Ecological Specialisation: Genomic Insights from the Diversification of Murine Rodents. Genome Biol Evol. 2021;13(7):evab103.
12. Schumacher J, Herlyn H. Correlates of evolutionary rates in the murine sperm proteome. BMC Evol Biol. 2018;18(1):35.
13. Winter EE, Goodstadt L, Ponting CP. Elevated Rates of Protein Secretion, Evolution, and Disease Among Tissue-Specific Genes. Genome Res. 2004;14(1):54-61.
14. Larracuente AM, Sackton TB, Greenberg AJ, Wong A, Singh ND, Sturgill D, et al. Evolution of protein-coding genes in Drosophila. Trends Genet. 2008;24(3):114-23.
15. Eddy EM. Male germ cell gene expression. Recent Prog Horm Res. 2002;57:103-28.
16. Chalmel F, Rolland AD, Niederhauser-Wiederkehr C, Chung SSW, Demougin P, Gattiker A, et al. The conserved transcriptome in human and

rodent male gametogenesis. Proc Natl Acad Sci U S A. 2007;104(20):8346-51.
17. Breed WG, Taylor J. Body mass, testes mass, and sperm size in murine rodents. J Mammal. 2000;81(3):758-68.
18. Wong A. The Molecular Evolution of Animal Reproductive Tract Proteins: What Have We Learned from Mating-System Comparisons? Int J Evol Biol. 2011;2011:908735.
19. Simmons LW, Fitzpatrick JL. Sperm wars and the evolution of male fertility. Reproduction (Camb). 2012;144(5):519-34.
20. Firman RC, Simmons LW. The frequency of multiple paternity predicts variation in testes size among island populations of house mice. J Evol Biol. 2008;21(6):1524-33.
21. Birkhead TR, Briskie JV, Møller AP. Male Sperm Reserves and Copulation Frequency in Birds. Behav Ecol Sociobiol. 1993;32(2):85-93.
22. Gómez Montoto L, Varea Sánchez M, Tourmente M, Martín-Coello J, Luque-Larena JJ, Gomendio M, et al. Sperm competition differentially affects swimming velocity and size of spermatozoa from closely related muroid rodents: head first. Reproduction. 2011;142(6):819-30.
23. Kopania EEK, Larson EL, Callahan C, Keeble S, Good JM. Molecular Evolution across Mouse Spermatogenesis. Mol Biol Evol. 2022;39(2):msac023.
24. Murat F, Mbengue N, Winge SB, Trefzer T, Leushkin E, Sepp M, et al. The molecular evolution of spermatogenesis across mammals. Nature. 2022;613:308–16.
25. Larson EL, Vanderpool D, Keeble S, Zhou M, Sarver BAJ, Smith AD, et al. Contrasting Levels of Molecular Evolution on the Mouse X Chromosome. Genetics. 2016;203(4):1841-57.
26. Dean MD, Clark NL, Findlay GD, Karn RC, Yi X, Swanson WJ, et al. Proteomics and Comparative Genomic Investigations Reveal Heterogeneity in Evolutionary Rate of Male Reproductive Proteins in Mice (Mus domesticus). Mol Biol Evol. 2009;26(8):1733-43.
27. Rowe KC, Achmadi AS, Esselstyn JA. A new genus and species of omnivorous rodent (Muridae: Murinae) from Sulawesi, nested within a clade of endemic carnivores. J Mammal. 2016;97(3):978-91.
28. Rowe KC, Achmadi AS, Fabre P-H, Schenk JJ, Steppan SJ, Esselstyn JA. Oceanic islands of Wallacea as a source for dispersal and diversification of murine rodents. J Biogeogr. 2019;46(12):2752-68.
29. Breed WG, Leigh CM, Peirce EJ. Reproductive biology of the mice and rats (family Muridae) in New Guinea—diversity and evolution. Rec Aust Mus. 2020;72(5):303-16.
30. Breed WG. Evolution of the spermatozoon in muroid rodents. J Morphol. 2005;265(3):271-90.
31. Gibbs RA, Weinstock GM, Metzker ML, Muzny DM, Sodergren EJ, Scherer S, et al. Genome sequence of the Brown Norway rat yields insights into mammalian evolution. Nature. 2004;428(6982):493-521.
32. Keane TM, Goodstadt L, Danecek P, White MA, Wong K, Yalcin B, et al. Mouse genomic variation and its effect on phenotypes and gene regulation. Nature. 2011;477(7364):289-94.
33. Green CD, Ma Q, Manske GL, Shami AN, Zheng X, Marini S, et al. A Comprehensive Roadmap of Murine Spermatogenesis Defined by Single-Cell RNA-Seq. Dev Cell. 2018;46(5):651-67.e10.
34. Firman RC. Of mice and women: advances in mammalian sperm competition with a focus on the female perspective. Philos Trans R Soc Lond, Ser B: Biol Sci. 2020;375(1813):20200082.
35. Steppan SJ, Schenk JJ. Muroid rodent phylogenetics: 900-species tree reveals increasing diversification rates. PLoS One. 2017;12(8):e0183070.
36. Roycroft E, MacDonald AJ, Moritz C, Moussalli A, Portela Miguez R, Rowe KC. Museum genomics reveals the rapid decline and extinction of Australian rodents since European settlement. Proceedings of the National Academy of Sciences. 2021;118(27):e2021390118.
37. Thomas GWC, Hahn MW. Referee: Reference Assembly Quality Scores. Genome Biol Evol. 2019;11(5):1483-6.
38. Hibbins MS, Gibson MJS, Hahn MW. Determining the probability of hemiplasy in the presence of incomplete lineage sorting and introgression. eLife. 2020;9:e63753.
39. Cooper N, Thomas GH, Venditti C, Meade A, Freckleton RP. A cautionary note on the use of Ornstein Uhlenbeck models in macroevolutionary studies. Biol J Linn Soc. 2016;118(1):64-77.
40. Dean MD, Ardlie KG, Nachman MW. The frequency of multiple paternity suggests that sperm competition is common in house mice (Mus domesticus). Mol Ecol. 2006;15(13):4141-51.
41. Ives AR, Garland T, Jr. Phylogenetic Logistic Regression for Binary Dependent Variables. Syst Biol. 2009;59(1):9-26.
42. Martins EP, Hansen TF. Phylogenies and the Comparative Method: A General Approach to Incorporating Phylogenetic Information into the Analysis of Interspecific Data. The American Naturalist. 1997;149(4):646-67.
43. Pagel M. Inferring the historical patterns of biological evolution. Nature. 1999;401(6756):877-84.
44. Hook KA, Wilke LM, Fisher HS. Apical Sperm Hook Morphology Is Linked to Sperm Swimming Performance and Sperm Aggregation in Peromyscus Mice. Cells. 2021;10(9):2279.
45. Good JM, Nachman MW. Rates of Protein Evolution Are Positively Correlated with Developmental Timing of Expression During Mouse Spermatogenesis. Mol Biol Evol. 2005;22(4):1044-52.
46. Endo T, Romer KA, Anderson EL, Baltus AE, de Rooij DG, Page DC. Periodic retinoic acid–STRA8 signaling intersects with periodic germ-cell competencies to regulate spermatogenesis. Proceedings of the National Academy of Sciences. 2015;112(18):E2347-E56.
47. Larson EL, Kopania EEK, Good JM. Spermatogenesis and the Evolution of Mammalian Sex Chromosomes. Trends Genet. 2018;34(9):722-32.
48. Yang Z. PAML 4: Phylogenetic Analysis by Maximum Likelihood. Mol Biol Evol. 2007;24(8):1586-91.
49. Kowalczyk A, Meyer WK, Partha R, Mao W, Clark NL, Chikina M. RERconverge: an R package for associating evolutionary rates with convergent traits. Bioinformatics. 2019;35(22):4815-7.
50. Saputra E, Kowalczyk A, Cusick L, Clark N, Chikina M. Phylogenetic Permulations: a statistically rigorous approach to measure confidence in associations in a phylogenetic context. Mol Biol Evol. 2021;38(7):3004–21.
51. Chikina M, Robinson JD, Clark NL. Hundreds of Genes Experienced Convergent Shifts in Selective Pressure in Marine Mammals. Mol Biol Evol. 2016;33(9):2182-92.
52. Bastian FB, Roux J, Niknejad A, Comte A, Fonseca Costa Sara S, de Farias TM, et al. The Bgee suite: integrated curated expression atlas and comparative transcriptomics in animals. Nucleic Acids Res. 2021;49(D1):D831-D47.
53. The UniProt Consortium. UniProt: the universal protein knowledgebase in 2021. Nucleic Acids Res. 2020;49(D1):D480-D9.
54. Du M, Yuan L, Zhang Z, Zhang C, Zhu M, Zhang Z, et al. PPP2R1B is modulated by ubiquitination and is essential for spermatogenesis. The FASEB

Journal. 2021;35(5):e21564.
55. Tan H, Wang W, Zhou C, Wang Y, Zhang S, Yang P, et al. Single-cell RNA-seq uncovers dynamic processes orchestrated by RNA-binding protein DDX43 in chromatin remodeling during spermiogenesis. Nat Commun. 2023;14(1):2499.
56. Breed WG. The spermatozoon of Eurasian murine rodents: Its morphological diversity and evolution. J Morphol. 2004;261(1):52-69.
57. Clark NL, Aagaard JE, Swanson WJ. Evolution of reproductive proteins from animals and plants. Reproduction. 2006;131(1):11-22.
58. Varea-Sánchez M, Tourmente M, Bastir M, Roldan ERS. Unraveling the Sperm Bauplan: Relationships Between Sperm Head Morphology and Sperm Function in Rodents. Biol Reprod. 2016;95(1):1–9.
59. Immler S, Moore HDM, Breed WG, Birkhead TR. By Hook or by Crook? Morphometry, Competition and Cooperation in Rodent Sperm. PLoS One. 2007;2(1):e170.
60. Moore H, Dvoráková K, Jenkins N, Breed W. Exceptional sperm cooperation in the wood mouse. Nature. 2002;418:174.
61. Firman RC, Simmons LW. Sperm competition and the evolution of the sperm hook in house mice. J Evol Biol. 2009;22(12):2505-11.
62. Tourmente M, Zarka-Trigo D, Roldan ERS. Is the hook of muroid rodent's sperm related to sperm train formation? J Evol Biol. 2016;29(6):1168-77.
63. Firman RC, Bentley B, Bowman F, Marchant FG-S, Parthenay J, Sawyer J, et al. No evidence of sperm conjugate formation in an Australian mouse bearing sperm with three hooks. Ecol Evol. 2013;3(7):1856-63.
64. Breed WG. Sperm head structure in the hydromyinae (rodentia:Muridae): A further evolutionary development of the subacrosomal space in mammals. Gamete Res. 1984;10(1):31-44.
65. Pitnick S, Markow TA. Male Gametic Strategies: Sperm Size, Testes Size, and the Allocation of Ejaculate Among Successive Mates by the Sperm-Limited Fly Drosophila pachea and Its Relatives. The American Naturalist. 1994;143(5):785-819.
66. Ramm SA, Schärer L. The evolutionary ecology of testicular function: size isn't everything. Biol Rev. 2014;89(4):874-88.
67. Cassaing J, Cervera S, Isaac F. Laboratory and field evidence of paternal care in the Algerian mouse (Mus spretus). J Ethol. 2009;28(1):7.
68. Firman RC, Gasparini C, Manier MK, Pizzari T. Postmating Female Control: 20 Years of Cryptic Female Choice. Trends Ecol Evol. 2017;32(5):368 - 82.
69. Mangels R, Tsung K, Kwan K, Dean MD. Copulatory plugs inhibit the reproductive success of rival males. J Evol Biol. 2016;29(11):2289-96.
70. Good JM, Wiebe V, Albert FW, Burbano HA, Kircher M, Green RE, et al. Comparative Population Genomics of the Ejaculate in Humans and the Great Apes. Mol Biol Evol. 2013;30(4):964-76.
71. Ramm SA, Oliver PL, Ponting CP, Stockley P, Emes RD. Sexual Selection and the Adaptive Evolution of Mammalian Ejaculate Proteins. Mol Biol Evol. 2008;25(1):207-19.
72. Dapper AL, Wade MJ. The evolution of sperm competition genes: The effect of mating system on levels of genetic variation within and between species. Evolution. 2016;70(2):502-11.
73. Mongue AJ, Hansen ME, Gu L, Sorenson CE, Walters JR. Nonfertilizing sperm in Lepidoptera show little evidence for recurrent positive selection. Mol Ecol. 2019;28:2517– 30.
74. Immler S, Calhim S, Birkhead TR. Increased Postcopulatory Sexual Selection Reduces the Intramale Variation in Sperm Design. Evolution. 2008;62(6):1538-43.
75. Breed WG, Ding X, Tuke J, Leigh CM. Morphological diversity of the spermatozoon and male reproductive tract in Australian Hopping mice, genus Notomys – is it determined by sexual selection? J Zool. 2020;311(3):194-203.
76. Bi K, Linderoth T, Vanderpool D, Good JM, Nielsen R, Moritz C. Unlocking the vault: next-generation museum population genomics. Mol Ecol. 2013;22(24):6018-32.
77. Shapiro B, Hofreiter M. Ancient DNA: methods and protocols: Springer; 2012.
78. Meyer M, Kircher M. Illumina sequencing library preparation for highly multiplexed target capture and sequencing. Cold Spring Harb Protoc. 2010;2010(6):pdb prot5448.
79. Roycroft EJ, Moussalli A, Rowe KC. Phylogenomics Uncovers Confidence and Conflict in the Rapid Radiation of Australo-Papuan Rodents. Syst Biol. 2019.
80. Hinrichs AS, Karolchik D, Baertsch R, Barber GP, Bejerano G, Clawson H, et al. The UCSC Genome Browser Database: update 2006. Nucleic Acids Res. 2006;34(suppl_1):D590-D8.
81. Bankevich A, Nurk S, Antipov D, Gurevich AA, Dvorkin M, Kulikov AS, et al. SPAdes: A New Genome Assembly Algorithm and Its Applications to Single-Cell Sequencing. J Comput Biol. 2012;19(5):455-77.
82. Slater GSC, Birney E. Automated generation of heuristics for biological sequence comparison. BMC Bioinformatics. 2005;6:31.
83. Katoh K, Misawa K, Kuma Ki, Miyata T. MAFFT: a novel method for rapid multiple sequence alignment based on fast Fourier transform. Nucleic Acids Res. 2002;30(14):3059-66.
84. Nguyen L-T, Schmidt HA, von Haeseler A, Minh BQ. IQ-TREE: A Fast and Effective Stochastic Algorithm for Estimating Maximum-Likelihood Phylogenies. Mol Biol Evol. 2014;32(1):268-74.
85. Kalyaanamoorthy S, Minh BQ, Wong TKF, von Haeseler A, Jermiin LS. ModelFinder: fast model selection for accurate phylogenetic estimates. Nat Methods. 2017;14(6):587-9.
86. Hoang DT, Chernomor O, von Haeseler A, Minh BQ, Vinh LS. UFBoot2: Improving the Ultrafast Bootstrap Approximation. Mol Biol Evol. 2017;35(2):518-22.
87. Yin J, Zhang C, Mirarab S. ASTRAL-MP: scaling ASTRAL to very large datasets using randomization and parallelization. Bioinformatics. 2019;35(20):3961-9.
88. Mendes FK, Hahn MW. Gene Tree Discordance Causes Apparent Substitution Rate Variation. Syst Biol. 2016;65(4):711-21.
89. Paradis E, Schliep K. ape 5.0: an environment for modern phylogenetics and evolutionary analyses in R. Bioinformatics. 2018;35(3):526-8.
90. Khabbazian M, Kriebel R, Rohe K, Ané C. Fast and accurate detection of evolutionary shifts in Ornstein–Uhlenbeck models. Methods Ecol Evol. 2016;7(7):811-24.
91. Tung Ho Ls, Ané C. A Linear-Time Algorithm for Gaussian and Non-Gaussian Trait Evolution Models. Syst Biol. 2014;63(3):397-408.
92. Pinheiro J BD, DebRoy S, Sarkar D, R Core Team. nlme: Linear and Nonlinear Mixed Effects Models. R package version 3.1-148. <URL: https://CRAN.R-project.org/package=nlme>. 2020.
93. Alexa A, Rahnenführer J, Lengauer T. Improved scoring of functional groups from gene expression data by decorrelating GO graph structure. Bioinformatics. 2006;22(13):1600-7.

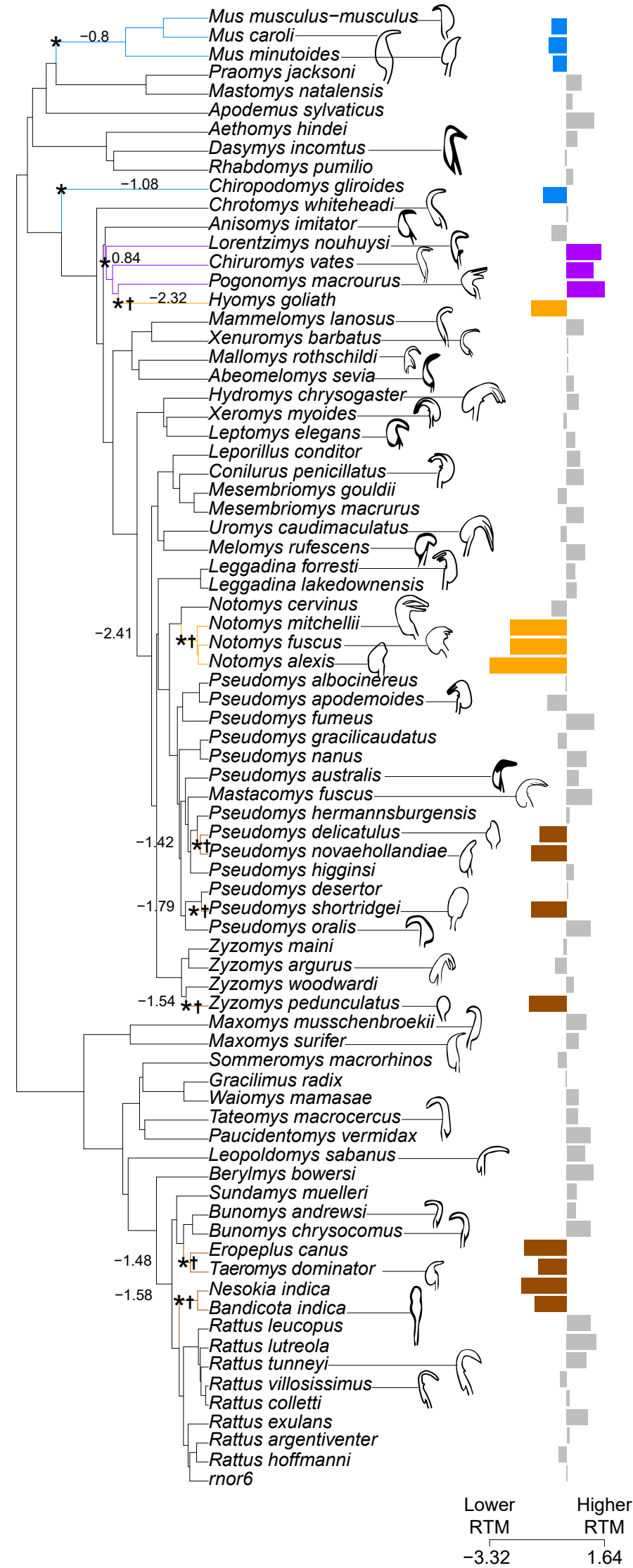
Mus musculus−musculus
Mus caroli
Mus minutoides
Praomys jacksoni
Mastomys natalensis
Apodemus sylvaticus
Aethomys hindei
Dasymys incomtus
Rhabdomys pumilio
Chiropodomys gliroides
Chrotomys whiteheadi
Anisomys imitator
Lorentzimys nouhuysi
Chiruromys vates
Pogonomys macrourus
Hyomys goliath
Mammelomys lanosus
Xenuromys barbatus
Mallomys rothschildi
Abeomelomys sevia
Hydromys chrysogaster
Xeromys myoides
Leptomys elegans
Leporillus conditor
Conilurus penicillatus
Mesembriomys gouldii
Mesembriomys macrurus
Uromys caudimaculatus
Melomys rufescens
Leggadina forresti
Leggadina lakedownensis
Notomys cervinus
Notomys mitchellii
Notomys fuscus
Notomys alexis
Pseudomys albocinereus
Pseudomys apodemoides
Pseudomys fumeus
Pseudomys gracilicaudatus
Pseudomys nanus
Pseudomys australis
Mastacomys fuscus
Pseudomys hermannsburgensis
Pseudomys delicatulus
Pseudomys novaehollandiae
Pseudomys higginsi
Pseudomys desertor
Pseudomys shortridgei
Pseudomys oralis
Zyzomys maini
Zyzomys argurus
Zyzomys woodwardi
Zyzomys pedunculatus
Maxomys musschenbroekii
Maxomys surifer
Sommeromys macrorhinos
Gracilimus radix
Waiomys mamasae
Tateomys macrocercus
Paucidentomys vermidax
Leopoldomys sabanus
Berylmys bowersi
Sundamys muelleri
Bunomys andrewsi
Bunomys chrysocomus
Eropeplus canus
Taeromys dominator
Nesokia indica
Bandicota indica
Rattus leucopus
Rattus lutreola
Rattus tunneyi
Rattus villosissimus
Rattus colletti
Rattus exulans
Rattus argentiventer
Rattus hoffmanni
rnor6
−0.8
−1.08
0.84
−2.32
−2.41
−1.42
−1.79
−1.54
−1.48
−1.58
Lower RTM
Higher RTM
−3.32
1.64

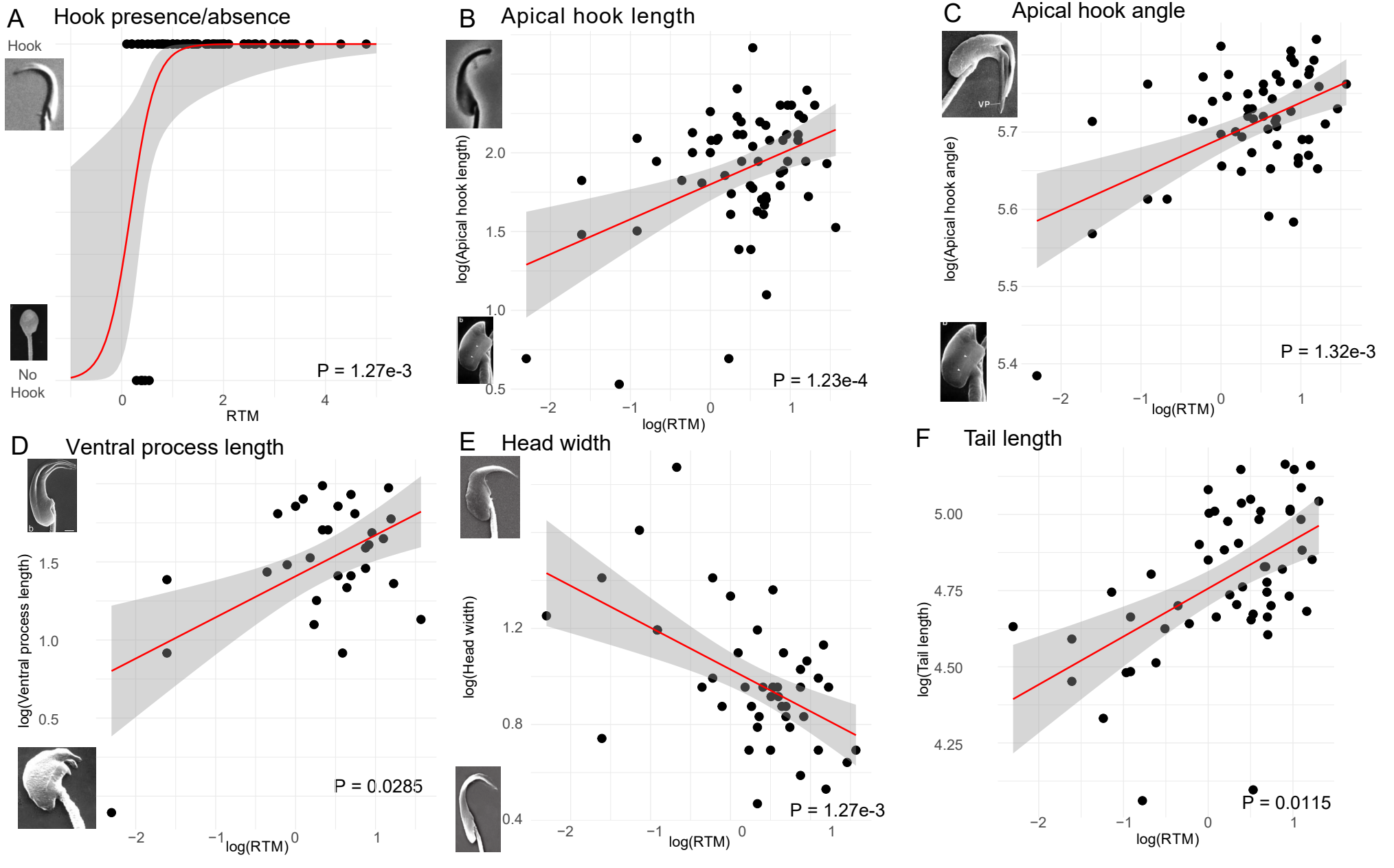
A
Hook presence/absence
Hook
No Hook
0
2
4
RTM
P = 1.27e-3
B
Apical hook length
log(Apical hook length)
2.0
1.5
1.0
0.5
−2
−1
0
1
log(RTM)
P = 1.23e-4
C
Apical hook angle
VP
log(Apical hook angle)
5.7
5.6
5.5
5.4
−2
−1
0
1
log(RTM)
P = 1.32e-3
D
Ventral process length
log(Ventral process length)
1.5
1.0
0.5
−2
−1
0
1
log(RTM)
P = 0.0285
E
Head width
log(Head width)
1.2
0.8
0.4
−2
−1
0
1
log(RTM)
P = 1.27e-3
F
Tail length
log(Tail length)
5.00
4.75
4.50
4.25
−2
−1
0
1
log(RTM)
P = 0.0115

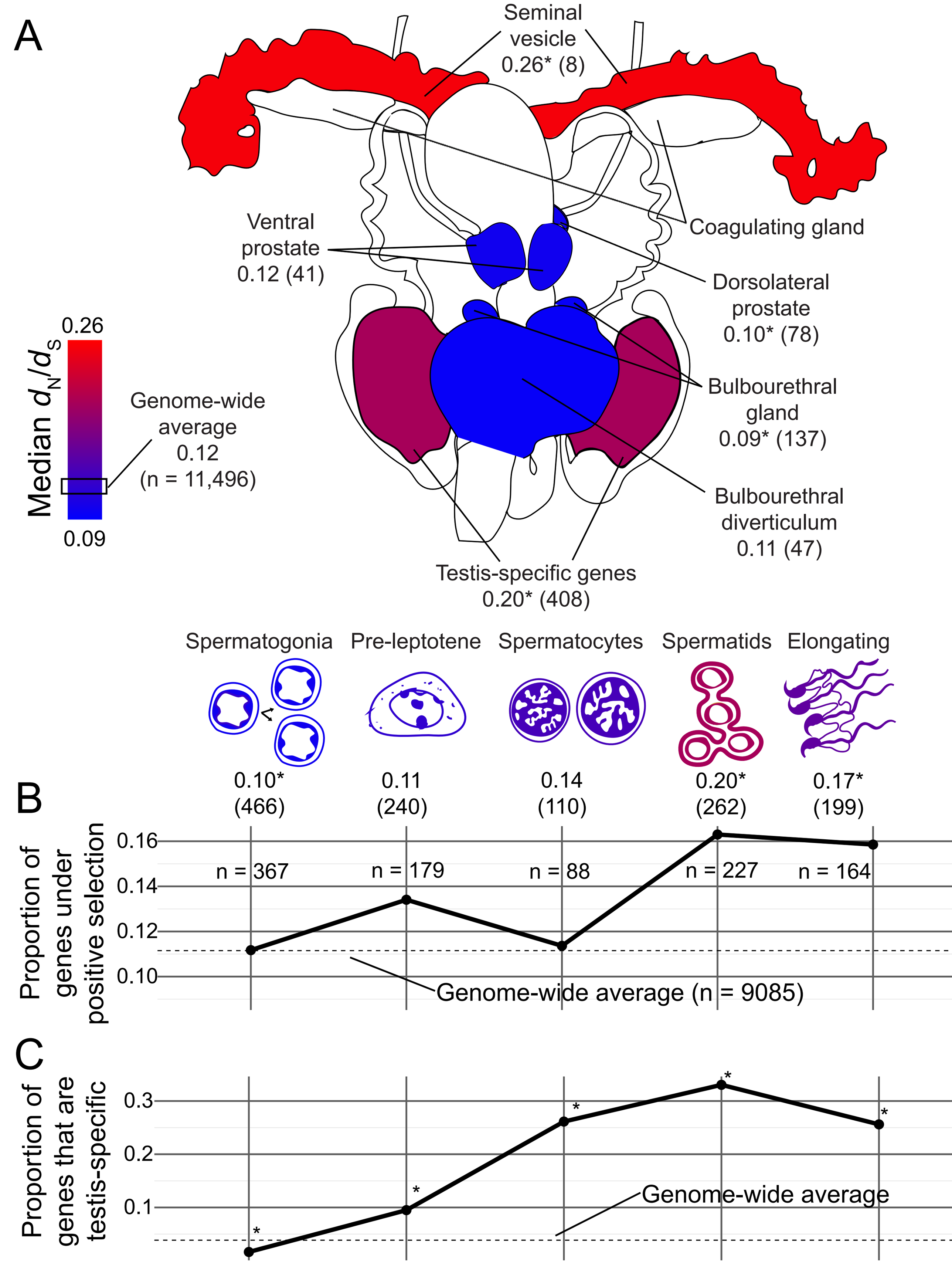
A
Seminal vesicle 0.26* (8)
Ventral prostate 0.12 (41)
Coagulating gland
Dorsolateral prostate 0.10* (78)
Bulbourethral gland 0.09* (137)
Bulbourethral diverticulum 0.11 (47)
Testis-specific genes 0.20* (408)
Median d_N/d_S
0.26
0.09
Genome-wide average 0.12 (n = 11,496)
Spermatogonia
Pre-leptotene
Spermatocytes
Spermatids
Elongating
0.10* (466)
0.11 (240)
0.14 (110)
0.20* (262)
0.17* (199)
B
Proportion of genes under positive selection
0.16
0.14
0.12
0.10
n = 367
n = 179
n = 88
n = 227
n = 164
Genome-wide average (n = 9085)
C
Proportion of genes that are testis-specific
0.3
0.2
0.1
Genome-wide average

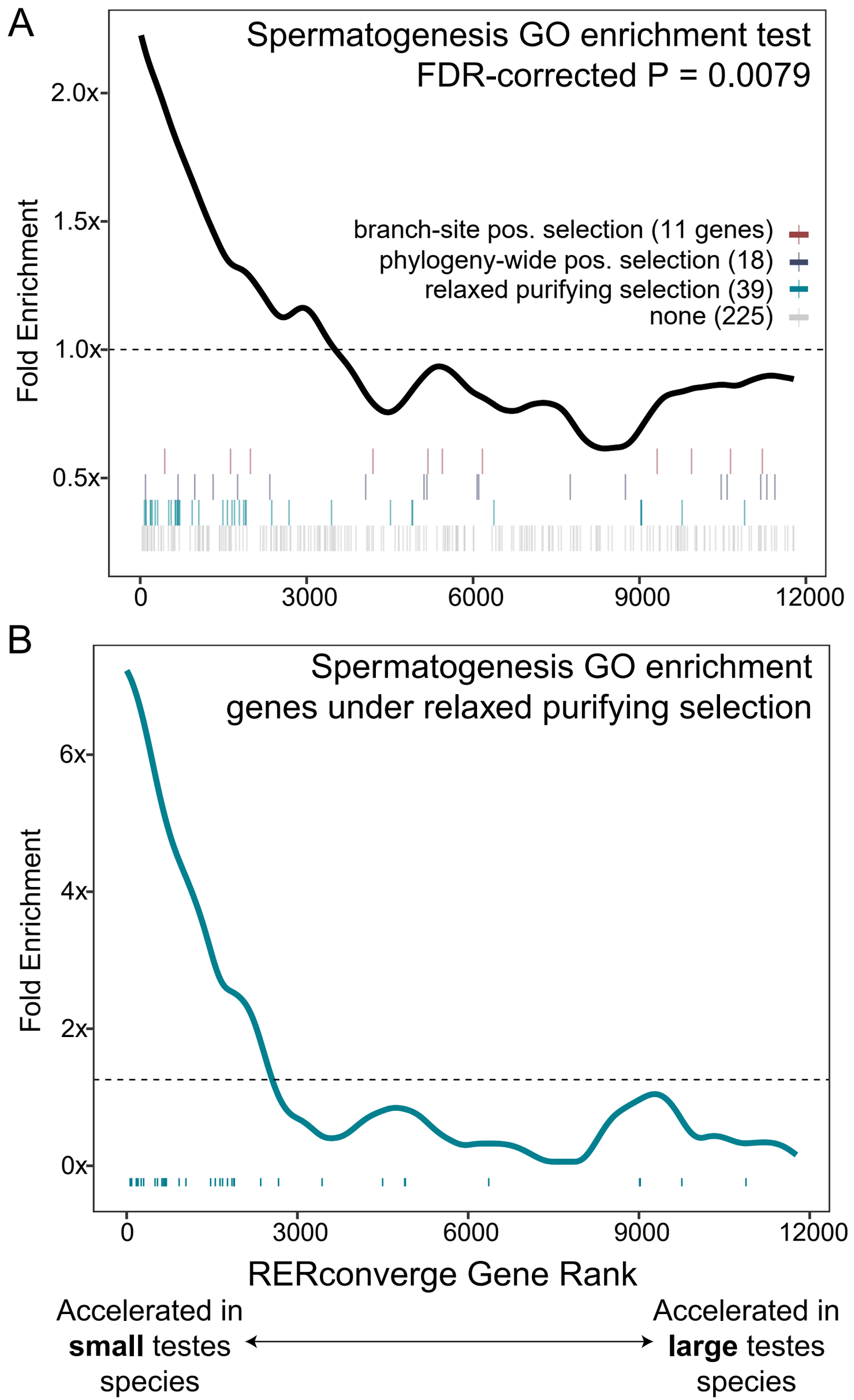
A
Spermatogenesis GO enrichment test
FDR-corrected P = 0.0079
Fold Enrichment
2.0x
1.5x
1.0x
0.5x
branch-site pos. selection (11 genes)
phylogeny-wide pos. selection (18)
relaxed purifying selection (39)
none (225)
0
3000
6000
9000
12000
B
Spermatogenesis GO enrichment
genes under relaxed purifying selection
Fold Enrichment
6x
4x
2x
0x
0
3000
6000
9000
12000
RERconverge Gene Rank
Accelerated in small testes species
Accelerated in large testes species